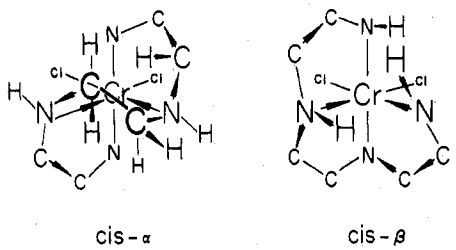

Figure 6. Steric blocking of *cis*-α- and *cis*-β-$[Cr(trien)Cl_2]^+$ ions trans to the chloride ligands.

of a solvated water molecule would thus be facilitated in the cis-β complex.

These considerations suggest that the dramatic difference between the rates of chloride aquation of the cis-α and cis-β isomers results from effective trans water attack in the cis-β isomer. The positive end of the ion's dipole must also be in the area trans to the anionic chlorides, so nucleophilic attack from that side is clearly favored. Nucleophilic water attack from the (electron-rich) cis side is usually invoked to account for the stereoretentive nature of most aquations at Cr(III) centers,[22] but the chemistry of *cis*-$[Cr(trien)Cl_2]^+$ is characterized by extensive geometric isomerization, especially in the presence of water (vide infra). Thus, cis attack of water need not be invoked for the aquation of *cis*-β-$[Cr(trien)Cl_2]^+$, and the results are more easily explained with a trans-attack model.

Acknowledgment. Acknowledgment is made to the doners of the Petroleum Research Fund, administered by the American Chemical Society, for the partial support of this research. We gratefully acknowledge the financial support of the National Science Foundation (Grant GP 27264) and the National Research Council of Italy (CNR). We also thank Mr. William Van Antwerp for assistance with the analysis of kinetic data and Dr. Fredrick Kull and the Department of Biological Sciences (SUNY Binghamton) for the use of their Cary 118 spectrophotometer.

Registry No. *cis*-$[Cr(en)_2Cl_2]ClO_4$, 15654-71-4; *cis*-α-[Cr(trien)Cl_2]ClO_4, 15738-64-4; *cis*-β-[Cr(trien)Cl_2]Cl, 57793-29-0; *cis*-β-[Cr(trien)Cl_2]ClO_4, 61587-73-3; *cis*-$[Cr(trien)Cl(H_2O)]^{2+}$, 16702-00-4; $[Cr(en)_2ox]ClO_4$, 42423-95-0; α-[Cr(trien)ox]ClO_4, 20097-09-0; α-[Cr(trien)ox]Br, 16060-20-1.

References and Notes

(1) Abbreviations used throughout: en, ethylenediamine; trien, triethylenetetramine; ox, oxalate dianion.
(2) *Inorg. Synth.*, **2**, 200 (1946).
(3) D. A. House and C. S. Garner, *J. Am. Chem. Soc.*, **88**, 2156 (1966).
(4) (a) "Gmelins Handbuch der Anorganishen Chemie", 8th ed, Chromium, Part C, Verlag Chemie, 1965, p 178; (b) E. Kyuno, M. Kamada, and N. Tanaka, *Bull. Chem. Soc. Jpn.*, **40**, 1848 (1967); (c) M. Cavanaugh, Ph.D. Thesis, Catholic University, 1973.
(5) C. Y. Hsu and C. S. Garner, *Inorg. Chim. Acta*, **1**, 17 (1967).
(6) J. W. Vaughn and D. J. Walkwitz, *Inorg. Chem.*, **5**, 1082 (1966).
(7) C. S. Garner and D. A. House, *Transition Met. Chem.*, **6**, 59 (1970).
(8) A. I. Vogel, "Practical Organic Chemistry", Wiley, New York, N.Y., 1957.
(9) P. Paoletti, M. Ciampolini, and L. Sacconi, *J. Chem. Soc.*, 3589 (1963).
(10) (a) A. M. Sargeson and G. H. Searle, *Inorg. Chem.*, **6**, 787 (1967); (b) A. W. Addison, R. D. Gillard, P. S. Sheridan, and L. R. H. Tipping, *J. Chem. Soc., Dalton Trans.*, 709 (1974); (c) D. U. Raichait and H. Taube, *Inorg. Chem.*, **11**, 999 (1972); H. Hartman and C. Buschbeck, *Z. Phys. Chem. (Frankfurt am Main)*, **11**, 120 (1957).
(11) *Inorg. Synth.*, **5**, 153 (1957).
(12) J. R. Perumareddi, *Coord. Chem. Rev.*, **4**, 73 (1969).
(13) A. M. Sargeson and G. H. Searle, *Inorg. Chem.*, **6**, 787 (1967).
(14) P. M. Gidney, R. D. Gillard, B. T. Heaton, P. S. Sheridan, and D. H. Vaughn, *J. Chem. Soc., Dalton Trans.*, 1462 (1973).
(15) A. A. Frost and R. G. Pearson, "Kinetics and Mechanism", 2nd ed, Wiley, New York, N.Y., 1961, p 162.
(16) See, for example, D. A. Palmer and D. W. Watts, *Inorg. Chim. Acta*, **6**, 197 (1972), and references therein.
(17) E. Zinato, P. Riccieri, and A. W. Adamson, *J. Am. Chem. Soc.*, **96**, 375 (1974).
(18) R. D. Archer, *Coord. Chem. Rev.*, **4**, 243 (1969).
(19) A. M. Sargeson and G. H. Searle, *Inorg. Chem.*, **6**, 2172 (1967).
(20) G. H. Searle and A. M. Sargeson, *Inorg. Chem.*, **12**, 1014 (1973).
(21) T. W. Swaddle, *Coord. Chem. Rev.*, **14**, 217 (1974).
(22) F. Basolo and R. G. Pearson, "Mechanisms of Inorganic Reactions", 2nd ed, Wiley, New York, N.Y., 1967.

Contribution from the Departments of Chemistry, Florida State University, Tallahassee, Florida 32306, and University of South Florida, Tampa, Florida 33620

Lattice Effects on Electron Resonance of Chromium(III) Complexes. Second-Neighbor Effects

B. B. GARRETT,* M. T. HOLBROOK, and J. A. STANKO

Received October 19, 1976 AIC60765P

Zero-field splitting parameters have been measured for $[Cr(NH_3)_5X]^{2+}$ in several $[M(NH_3)_5Y]Z_2$ hosts with X = Cl, Br; Y = Cl, Br; Z^- = Cl^-, Br^-, I^-, NO_3^-; and M = Co, Rh, Ir. The guest–host combinations and comparisons were chosen to determine the magnitude and regularities of second-near-neighbor effects in this series of isomorphous orthorhombic hosts. Bound-halogen substitution (Y) in the second shell has about one-tenth the near-neighbor effect on the axial zero-field parameter but gives similar effects to those of the first shell (Z) on the rhombic parameter. Metal ion substitution in the second shell gives smaller effects on both axial and rhombic parameters but temperature variation of these systems reveals new information about temperature-dependent lattice effects. The second-shell effects are correlated with previously proposed models for lattice interactions in this type of host. The $[Rh(NH_3)_5Cl](NO_3)_2$ host system displays a reversible transformation to a lattice with two or more guest sites at low temperatures and undergoes smooth decomposition at high temperatures.

Introduction

We have studied lattice effects on the electron resonance spectra of molecular ions in crystals by a variety of comparisons albeit inadvertently at times.[1-6] The primary effect appears in the zero-field splitting tensor for d^3 and d^5 ions with only small **g**-tensor variations.[2,5] An isomorphous series of orthorhombic lattices[5,7,8] with the general formula $[M(NH_3)_5Y]Z_2$ where M = Co, Rh, or Ir, Y = Cl or Br, and Z^- = Cl^-, Br^-, I^-, or NO_3^- has been used to study the effect of nearest-neighbor, Z, variations on the paramagnetic $[Cr(NH_3)_5X]^{2+}$ guests (X = Cl or Br) in the analogous cobalt hosts, X = Y. A perspective view of the lattice is shown in Figure 1. Room-temperature lattice comparisons[5] and extensive temperature variation[6] studies in the range from 4 to 570 K have demonstrated the existence of a 20% lattice effect on the axial zero-field splitting parameter, *D*, and large variations of the rhombic parameter, *E*. Both *D* and *E* appear to respond to different lattice mechanisms in the low- and

* To whom correspondence should be addressed at Florida State University.

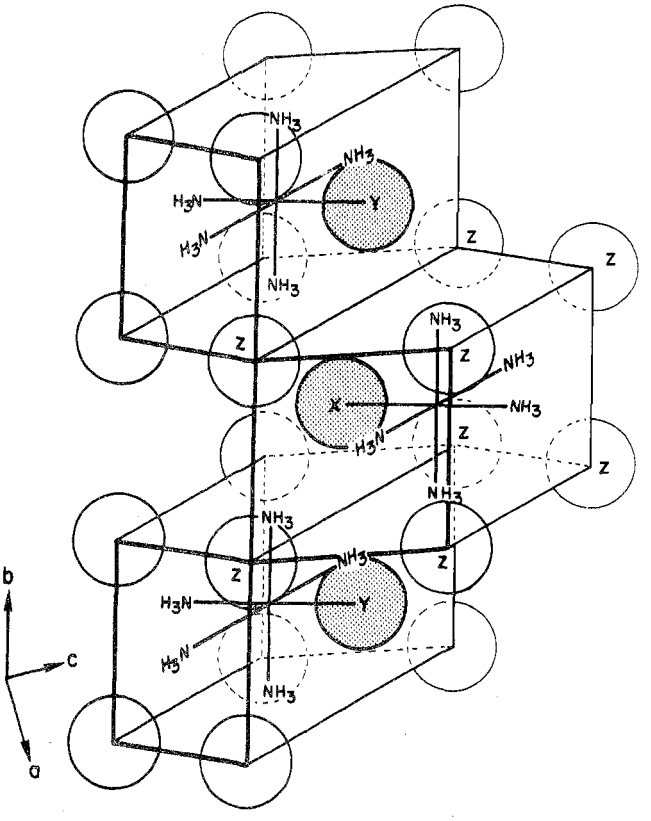

Figure 1. Perspective view of the immediate surroundings of the paramagnetic guest complex $[Cr(NH_3)_5X]$ in the orthorhombic diamagnetic hosts $[M(NH_3)_5Y]Z_2$. Note the outline of the distorted cube of eight Z ions about each body-centered complex. Also note the staggered X, Y, Z stacking along the *b* axis.

high-temperature regimes and the dominant effects for the two parameters have not been shown to correspond. The effect of the nearest-neighbor (first shell) counterions, Z, on *D* and the high-temperature falloff of the axial parameter have been rationalized in terms of a mechanism which envisions the bound halide X of the guest as being pushed away from the chromium ion (with concomitant axial crystal field reduction) by the nearest-neighbor *Z* ions. Changes in the lattice which increase the effective size of the Z ions give reductions in the magnitude of *D*. The rhombic parameter *E* varies at low temperature but approaches a constant, lattice-specific, nonvanishing value at higher temperatures. This behavior was presumed to arise from specific nearest-neighbor interactions with the guest ammine ligands at low temperatures giving way to a cavity shape effect at higher temperatures. The shape of the cavity formed by nearest-neighbor counterions is imposed on the guest through the electrostatic potential and a channeling of guest ion motions.[6]

In the present study we have made variations of the second near neighbors or second shell by preparing $[Cr(NH_3)_5X]$: $[M(NH_3)_5Y]Z_2$ with X, Y = Cl, Br, M = Co, Rh, Ir, and Z = Cl^-, Br^-, I^-, NO_3^-. The temperature dependences of the rhodium and iridium hosts have been examined as well. Variations due to the second shell are not as large as first-shell effects and depend on which Z ion is in the first shell.

Methods and Results

The cobalt and rhodium host samples were prepared in a similar manner to those in previous reports.[5,6] A filtered saturated solution of the host, contaminated with about 2% of the paramagnetic guest compound, was placed in an ice bath and a stream of warm, dry air was drawn across the surface overnight. The resulting well-formed crystals were filtered, washed with a small amount of ethanol and acetone, dried in air, ground to a very fine powder, and sealed in thin quartz capillaries. Each cobalt and rhodium sample was prepared independently at least twice with reproducible results. The iridium samples were prepared from a small chromium-doped single crystal[9] of $[Ir(NH_3)_5Cl]Cl_2$ which was ground, measured, and recrystallized as the bromide salt for measurements. The sample was lost in subsequent attempts at recrystallization with other counterions.

Room-temperature electron resonance spectra were obtained at both 35 and 9 GHz and variable-temperature spectra were obtained at the lower frequency using a Varian E12 spectrometer and a Spectromagnetic Industries NMR Model 5200 gauss meter. Frequencies were measured before, during, and after each spectrum by measuring the resonant field of a DPPH sample with the E272B field-frequency lock. Line positions were reproducibly measured within a few tenths of 1 G and fitted to the spin Hamiltonian

$$\mathcal{H} = \beta H \cdot g \cdot S + D'[S_z^2 - S(S+1)/3] + E'[S_x^2 - S_y^2]$$

with D (gauss) = $D'/g_z\beta$; E (gauss) = $E'/g_\perp\beta$. The zero-field parameters are reported in gauss for convenience.[6] An iterative procedure involving a matrix diagonalization at each resonant field gave excellent fits of all nine principal-axis resonances of the $S = {}^3/_2$ spectra as illustrated by three typical examples in Table I. A sampling of 25 spectra with good line shapes and no superposition of lines gave an average deviation of 0.63 G for all of the lines while 10 spectra with overlapping lines gave an average deviation of 2.1 G with most of the error accumulated from the poorly resolved lines. The effect of incomplete resolution can be seen from the relatively poor fit of the center lines in the *x* and *y* spectra of the rhodium host samples in Table I. A line shape analysis could significantly improve these fits[2] but was not warrented in this work. Again[6] the *g* factors did not show significant variations beyond those introduced by spectrometer frequency fluctuations. Complete tabulations of the best fit spin-Hamiltonian parameters for the spectra reported in this paper are given elsewhere.[10]

A comparison of zero-field parameters for $[Cr(NH_3)_5X]^{2+}$ (X = Cl, Br) in lattices differing in the bound halide of the second shell is given in Table II. The hosts $[Co(NH_3)_5Y]Z_2$ with Y = Cl and Br for each Z^- = Cl^-, Br^-, I^-, and NO_3^- compared horizontally show second-shell effects of 40 G or less in *D* which are significantly smaller than the ~200-G variations with changes in the nearest neighbors seen from vertical comparisons in Table II. A bound chloride instead of bromide in the second shell gives larger axial parameters in six of the eight comparisons with the others showing no change. The rhombic parameter *E* shows second-shell effects of similar size (but inconsistent sign) to those seen for *D*. The effect of substituting water for the trans ammine in the second near neighbor of the host may be seen by comparing the first and last entries of the last column in Table II. The change in hydrogen bonding probably dominates this comparison.

The next to the last entry in Table II almost certainly represents a variation within the first shell about the guest ion. This spectrum arose as a second spectrum in the samples of $[Cr(NH_3)_5Cl]^{2+}$ in $[Co(NH_3)_5Br]Cl_2$ and increased in intensity with longer crystal growth times. The second spectrum develops because of hydrolysis of the host cations to yield bromide ions which are preferentially incorporated into the growing crystal. This explanation was verified by deliberate contamination of the crystal-growing solution with 1% bromide ions which produced a significant amplification of the second spectrum. There are four types of nearest-neighbor sites available on the corners of the eightfold anion "cube" about the body-centered guest ion, two sites adjacent to the bound chloride of the guest ion and two on the opposite side of the equatorial plane of the guest (see Figure 1). One face of the

Table I. Typical Experimental Data and Spin-Hamiltonian Fits for Powder Electron Resonance

Sample	Cr:$[Ir(NH_3)_5Cl]Br_2$	Cr:$[Rh(NH_3)_5Cl]Cl_2$	Cr:$[Rh(NH_3)_5Cl]I_2$
T, K	77	410	297
ν,[a] GHz	9.1344	9.1483	9.5274
g_z	1.9847	1.9852	1.9839
g_y	1.9856	1.9855	1.9858
g_x	1.9857	1.9862	1.9869
D, G	848.7	940.3	697.5
E, G	9.3	45.8	84.0

Resonant Fields[b]

H along	Exptl	Calcd	Exptl	Calcd	Exptl	Calcd
z	1591.1	1591.1	1417.1	1417.1	2040.4	2040.4
	3288.2	3288.2	3290.1	3290.5	3425.0	3425.0
	4985.6	4985.6	5173.0	5173.0	4825.8	4825.8
y	4149.7	4150.3	4352.8	4353.0	4369.0	4370.5
	3118.3	3116.4	3096.7	3095.7	3346.4	3342.3
	2448.0	2447.5	2274.8	2274.6	2501.2	2499.7
x	4093.5	4094.0	4076.3	4076.5	3863.2	3864.7
	3107.9	3108.7	3056.0	3052.7	3291.0	3287.5
	2501.5	2501.0	2531.3	2531.1	2993.3	2991.8
Av dev[b]		0.5		0.6		1.5

[a] Frequency determined from external DPPH resonance in a Varian E272B field-frequency lock. [b] All resonant fields and deviations are given in gauss.

Table II. Zero-Field Splitting Variations with Changes in the Second Shell: $[Cr(NH_3)_5X]$ in $[Co(NH_3)_5Y]Z_2$ Hosts[a]

X in guest	Z in host	Y = Br		Y = Cl	
		D	E	D	E
Cl	Cl	940	86	950[b]	47
Cl	Br	849	45	852[b]	6
Cl	I	680	34	702[b]	85
Cl	NO_3	767	6	767[b]	4
Br	Cl	2276[b]	37	2317	17
Br	Br	2224[b]	23	2255	47
Br	I	2182[b]	111	2223	135
Br	NO_3	2127[b]	8	2143	9
Cl	Cl (Br)	1001[c]	72		
Cl	Cl[d]			1128	14

[a] All data in this table are taken from room-temperature 35-GHz spectra. D and E are in units of gauss. [b] Data from ref 1. [c] This spectrum appears due to host cation hydrolysis with resultant substitution of one or more chloride ions by bromide ions in the nearest-neighbor positions to the paramagnetic guest in the lattice $[Co(NH_3)_5Br]Cl_2$. See text. [d] The host cation is *trans*-$[Co(NH_3)_4ClH_2O]^{2+}$ which is expected to be similar to $[Co(NH_3)_5Cl]Cl_2$, but these lattices have not been shown to be isomorphous. Data are from ref 3.

approximate cube of anions is related to the other face by a mirror plane normal to the b axis and containing M, X, and three nitrogens. Several possibilities exist in the next layer of anion sites and bromide ions should produce different spectra for each type of site but only one bromide-perturbed spectrum has yet been observed. Identification of the bromide perturbation site, the nature of the site selectivity, and elucidation of lattice effects with such perturbations will be examined another time.

Another second-shell comparison is accomplished by varying the metal ion in the host lattice. A prior comparison[1] of the host $[Co(NH_3)_5Cl]Cl_2$ with the rhodium analogue had revealed no essential difference in these hosts at room temperature (and this was verified here) but further studies were indicated by our more recent lattice effect observations.[5,6] The temperature dependence of the zero-field splitting parameters of $[Cr(NH_3)_5Cl]^{2+}$ in $[M(NH_3)_5Cl]Cl_2$ hosts (M = Co, Rh, Ir) are compared in Figure 2 and Table III. The cobalt and rhodium hosts have almost identical behavior above 200 K but

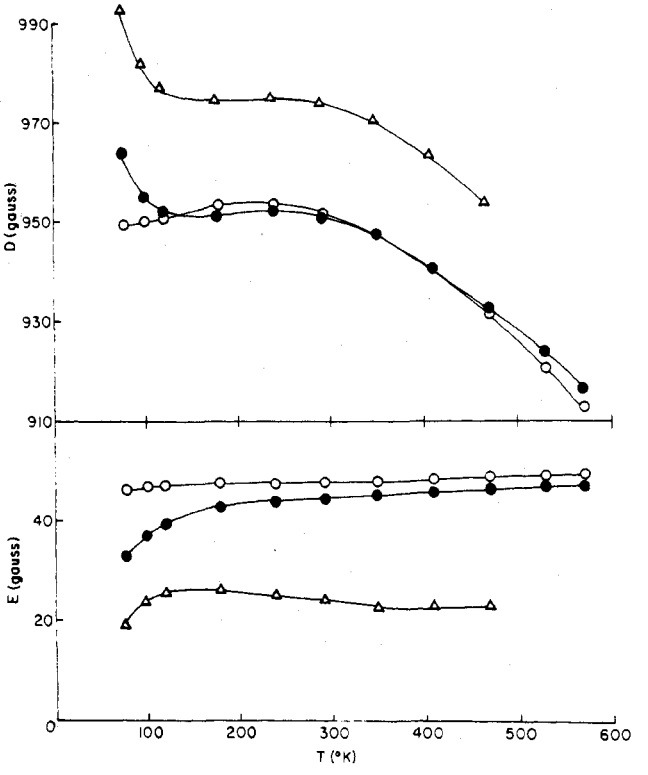

Figure 2. Temperature dependence of the zero-field splitting parameters for $[Cr(NH_3)_5Cl]^{2+}$ in $[M(NH_3)_5Cl]Cl_2$ hosts: M = cobalt (○), rhodium (●), and iridium (△).

both D and E diverge at lower temperatures for these systems. Except for a 23-G shift to larger values, the curve for D in the iridium host is superimposable on the rhodium curve. The rhombic parameter E shows a significant low-temperature variation for Rh and Ir hosts in contrast to the virtually temperature-independent behavior in the cobalt host. The low-temperature variations of D and E are well correlated for both Rh and Ir hosts. Similar comparison with bromide counterions, Z, are shown in Figure 3 and Table IV. Only three temperatures were examined for $[Rh(NH_3)_5Cl]Br_2$ because these established that there was no essential difference

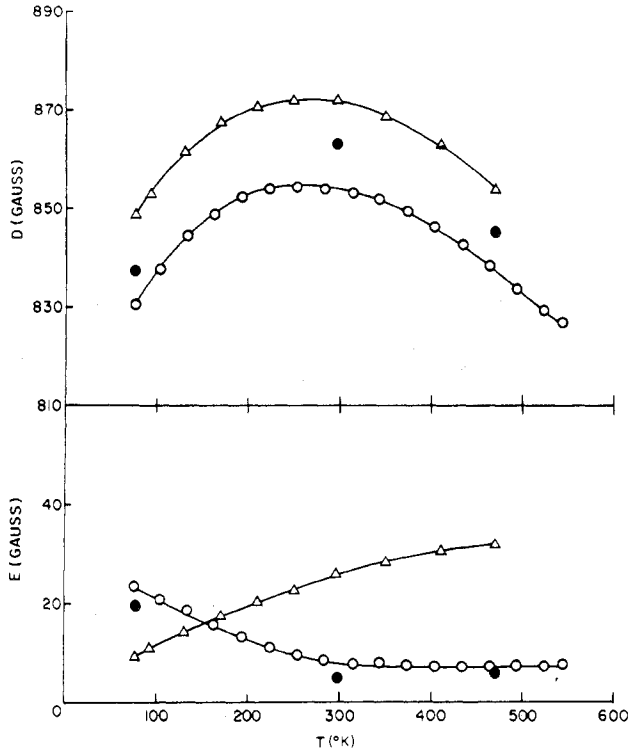

Figure 3. Temperature dependence of the zero-field splitting parameters for $[Cr(NH_3)_5Cl]^{2+}$ in $[M(NH_3)_5Cl]Br_2$ hosts: M = cobalt (○), rhodium (●), and iridium (△).

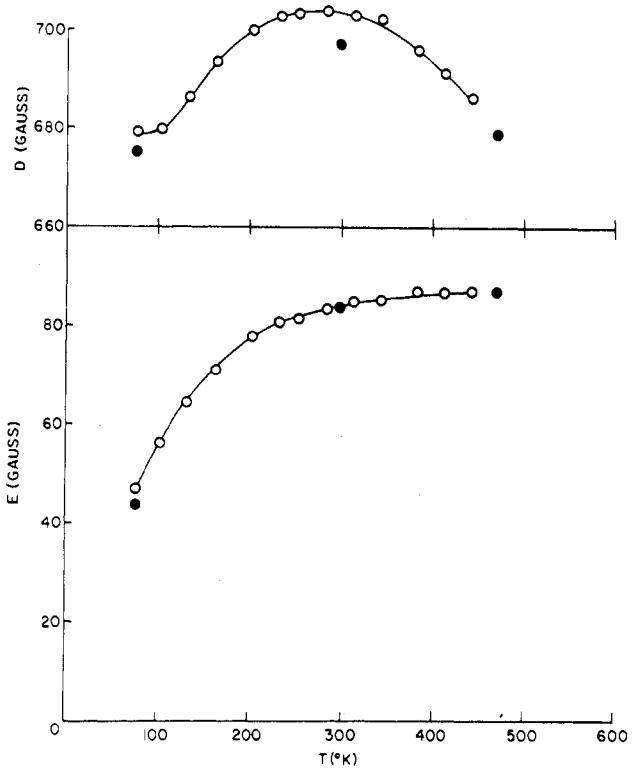

Figure 4. Comparison of the temperature dependence of the zero-field splitting parameters of $[Cr(NH_3)_5Cl]^{2+}$ in $[Co(NH_3)_5Cl]I_2$ (○) and $[Rh(NH_3)_5Cl]I_2$ (●) hosts.

Table III. Temperature Variation of the Zero-Field Splitting Parameters of $[Cr(NH_3)_5Cl]$ in Several Isomorphous Hosts Illustrating the Effect of Second-Neighbor Interactions

	Host					
	$[Co(NH_3)_5Cl]Cl_2$		$[Rh(NH_3)_5Cl]Cl_2$		$[Ir(NH_3)_5Cl]Cl_2$	
T, K	D, G	E, G	D, G	E, G	D, G	E, G
77	949.4	46.2	963.6	33.0	992.8	19.3
100	949.9	46.9	955.2	37.1	982.1	23.9
120	950.6	47.0	952.1	39.4	977.2	25.5
180	953.2	47.5	951.1	42.7	974.4	26.2
240	953.1	47.4	952.0	43.9	974.7	25.1
293	951.2	47.7	950.7	44.6	973.5	24.3
350	947.0	47.7	946.9	45.1	969.9	22.8
410	940.1	48.3	940.3	45.8	962.7	22.9
470	931.2	48.7	932.1	46.4	953.3	23.1
530	920.5	49.1	923.7	46.9		
570	912.7	49.2	916.3	47.3		

from the analogous cobalt host. The D curve of the iridium host is identical with that of cobalt host except for a 17.6 ± 1 G shift to larger D's. The rhombic parameter for the $[Ir(NH_3)_5Cl]Br_2$ host has the same slope as but opposite sign of that for the cobalt host below about 250 K. At higher temperatures E for the $[Co(NH_3)_5Cl]Br_2$ host reaches a constant value of 7.3 G while the iridium lattice rhombic parameter did not achieve a high-temperature limit in the range studied. Lattices with iodide counterions showed virtually identical behavior for cobalt and rhodium complexes in the second shell as shown in Figure 4. The $[Ir(NH_3)_5Cl]I_2$ was not studied.

The spectra of $[Cr(NH_3)_5Cl]^{2+}$ in $[Rh(NH_3)_5Cl](NO_3)_2$ host were also examined for a second-neighbor-effect comparison with the cobalt analogue. The rhodium host (Figure 5) shows the same type of sharp low-temperature transition seen previously[6] in cobalt hosts but at a lower temperature. The cobalt host transition begins at about 155 K when approached from the high-temperature side. It is reversible, and the spectra can be measured throughout the transition region. The rhodium host shows an even sharper onset of the transition at about 138 K, and it is also reversible. In contrast, however, the spectra in the rhodium host show severe line broadening

Table IV. Temperature Variation of the Zero-Field Splitting Parameters for $[Cr(NH_3)_5Cl]$ in Several Hosts Illustrating Second-Neighbor Effects

$[Ir(NH_3)_5Cl]Br_2$ host			$[Rh(NH_3)_5Cl](NO_3)_2$[a] host			$[Rh(NH_3)_5Cl]Br_2$ host			$[Rh(NH_3)_5Cl]I_2$ host		
T, K	D, G	E, G	T, K	D, G	E, G	T, K	D, G	E, G	T, K	D, G	E, G
77	848.7	9.3	110	972.6	173	77	837.3	19.8	77	675.6	44.0
93	853.4	10.9	120	937.2	102.5	297	863.4	5.1	297	697.5	84.0
130	861.5	14.1	130	841.1	16.2	470	845.5	6.1	470	679.2	87.2
170	867.4	17.3	140	793.0	5.9						
210	870.7	20.3	150	790.0	4.8						
250	872.1	22.6	180	785.7	3.8						
296	872.1	25.9	210	781.8	3.4						
350	868.6	28.2	240	777.9	2.9						
410	863.1	30.4	296	769.1	2.2						
470	854.1	31.9	350	760.7	2.1						
			410	750.3	2.2						

[a] The available temperature range for $[Rh(NH_3)_5Cl](NO_3)_2$ was limited by excessive broadening and further splittings at lower temperatures and decomposition at higher temperatures. At 470 K the signal intensity decayed smoothly with a half-life of 3.9 min.

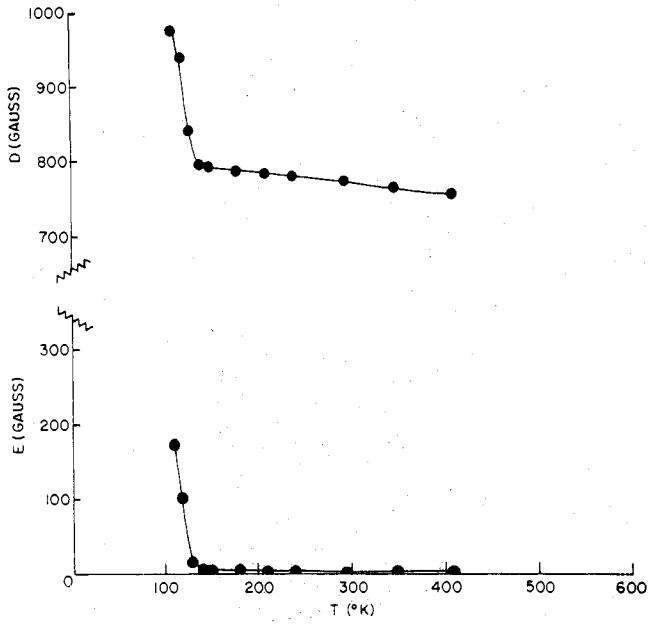

Figure 5. Zero-field splitting parameters for $[Cr(NH_3)_5Cl]^{2+}$ in $[Rh(NH_3)_5Cl](NO_3)_2$ host—temperature variation.

in the transition region preventing measurements below 110 K. At lower temperatures two distinct spectra with different spin-Hamiltonian parameters can be discerned, but even at 77 K (our lowest accessible temperature) these spectra could not be resolved sufficiently for measurement. Above the transition the $[Rh(NH_3)_5Cl](NO_3)_2$ host displays the same linear decrease of D with temperature which was previously seen with nitrate counterions.[6] Another interesting observation with this system was the very smooth exponential decay of the EPR spectrum when the temperature was raised to 470 K. This decomposition was observable over a range of temperatures with varying decay rates. Several such thermal decompositions will be described in a future communication.

Discussion

Previous studies of lattice effects on the zero-field splitting of $[Cr(NH_3)_5X]$ guests in $[M(NH_3)_5Y]Z_2$ hosts have demonstrated that the primary lattice effect on the axial parameter, D, involves displacement of the bound halide, X, by touching repulsions from the near-neighbor counterions, Z.[5,6] Smaller Z ions force the X ligand off the paramagnetic center thereby giving larger axial splittings. This effect may be called a lattice-squeezing mechanism. Temperature variations of the zero-field splittings have indicated that three separate lattice mechanisms exist including separate low- and high-temperature effects on the axial parameter and an independent low-temperature effect on the rhombic splitting. The second-near-neighbor effects reported here are supportive of the lattice-squeezing mechanism and comparison of temperature variations for different second-neighbor lattices more clearly illustrates the existence of the three previously postulated dynamic effects. Two types of second-shell variations were made in the present study including comparisons of Br and Cl in the bound-halide position Y and Co, Rh, and Ir interchange in the host. Both types of substitution give ambient-temperature zero-field parameter variations of 50 G or less for the same first-shell counterion in contrast to the 200-G changes observed with different first-shell counterions.

The substitution of Br for Cl in the bound-halide (Y) position of the host $[Co(NH_3)_5Y]Z_2$ gave consistently smaller values of the axial parameter, D, in accord with the lattice-squeezing mechanism. The agreement can be seen from the following considerations. The principal effect of replacing Cl by Br in this series of lattices is an expansion along the b lattice direction to accommodate the larger bromine. The a and c axes of the unit cell remain the same or decrease slightly to maintain a constant unit cell volume (see Table II of ref 5). This illustrates that the primary second-neighbor bound-halide lattice contacts are with the Z counterions and such repulsions would tend to separate Z counterions which are holding the bound halide X of the paramagnetic guest away from the metal ion. Thus the effect of increasing size of the bound halide Y in the second shell is to allow the bound halide X to relax onto the paramagnetic center which reduces the anisotropy and consequently D at that site. This effect should be more pronounced with larger bromine instead of chlorine at the bound-halide site X on the paramagnetic center. This comparison can be seen in Table II where for the same host system pairs [Y = Cl, Br] the change in D is at least twice as large for X = Br as for X = Cl. The effect of host bound-halide substitution should be smallest with the large and apparently rotating nitrate ion at the Z site and this is observed. The effects of Y interchange on the rhombic parameter, E, are as large as the changes seen in D and of about the same magnitude as the E parameter itself. The variations in the E parameter show no correlation with ion size at either the Y or Z site of the host.

The most remarkable feature of the host lattice metal ion substitution comparisons and their temperature dependences is the similarity of the data for all three metal ions. With chloride counterions (Figure 2) both rhodium and iridium have large D's at low temperature which fall off in concert with an increase in the rhombic parameter but the parameter curves for all three metal ion systems are superimposable at higher temperatures. With bromide counterions (Figure 2) all three D curves are superimposable and iridium differs in the rhombic parameter only by having an opposite sign of the temperature-dependent component. With iodide counterions only cobalt and rhodium were studied and the curves in Figure 3 are virtually identical. A summary of the metal ion substitution results is that these second-shell effects are small and appear to reflect only the size of the host cation. Cobalt(III) and rhodium(III) are essentially the same size with iridium(III) being slightly larger. The temperature dependences strongly reinforce the earlier study[6] which inferred the existence of two or three temperature-dependent processes in this type of lattice. Every system studied to date has a high-temperature falloff of the axial parameter. There is a low-temperature process which affects both D and E and appears to level off by about 300 K. The obvious correlation of the temperature variations of D and E in Figures 1–3 makes it possible to associate the axial and rhombic low-temperature phenomena. This was not apparent in the previous study.[6]

Registry No. $[Co(NH_3)_5Br]Cl_2$, 13601-38-2; $[Co(NH_3)_5Br]Br_2$, 14283-12-6; $[Co(NH_3)_5Br]I_2$, 14591-70-9; $[Co(NH_3)_5Br](NO_3)_2$, 21333-43-7; $[Co(NH_3)_5Cl]Cl_2$, 13859-51-3; $[Co(NH_3)_5Cl]Br_2$, 13601-43-9; $[Co(NH_3)_5Cl]I_2$, 37922-32-0; $[Co(NH_3)_5Cl](NO_3)_2$, 13842-33-6; $[Cr(NH_3)_5Cl]^{2+}$, 14482-76-9; $[Cr(NH_3)_5Br]^{2+}$, 22289-65-2; $[Ir(NH_3)_5Cl]Br_2$, 29928-29-8; $[Rh(NH_3)_5Cl]Cl_2$, 13820-95-6; $[Rh(NH_3)_5Cl]I_2$, 29928-28-7; $[Ir(NH_3)_5Cl]Cl_2$, 15742-38-8; $[Rh(NH_3)_5Cl](NO_3)_2$, 21264-83-5; $[Rh(NH_3)_5Cl]Br_2$, 29928-27-6.

References and Notes

(1) L. E. Mohrmann, Jr., and B. B. Garrett, *Inorg. Chem.*, **13**, 357 (1974).
(2) E. W. Stout, Jr., and B. B. Garrett, *Inorg. Chem.*, **12**, 2565 (1973).
(3) G. M. Cole, Jr., and B. B. Garrett, *Inorg. Chem.*, **13**, 2680 (1974).
(4) S. J. Baker and B. B. Garrett, *Inorg. Chem.*, **13**, 2683 (1974).
(5) M. T. Holbrook and B. B. Garrett, *Inorg. Chem.*, **15**, 150 (1976).
(6) B. B. Garrett and M. T. Holbrook, *Inorg. Chem.*, **15**, 2609 (1976).
(7) C. D. West, *Z. Kristallogr., Kristallgeom., Kristallphys., Kristallchem.*, **91**, 181 (1935); R. S. Evans, E. A. Hopcus, J. Bordner, and A. F. Schreiner, *J. Cryst. Mol. Struct.*, **3**, 235 (1973).
(8) G. G. Messmer and E. L. Amma, *Acta Crystallogr., Sect. B*, **24**, 412 (1968).
(9) J. A. Stanko, Ph.D. Thesis, University of Illinois, 1966.
(10) M. T. Holbrook, Ph.D. Dissertation, Florida State University, 1976.